



PERGAMON

Available online at [www.sciencedirect.com](http://www.sciencedirect.com)

SCIENCE @ DIRECT®

Solid State Communications 126 (2003) 629–633

solid  
state  
communications

[www.elsevier.com/locate/ssc](http://www.elsevier.com/locate/ssc)

## The octa-twin tetraleg ZnO nanostructures

Ying Dai<sup>a</sup>, Yue Zhang<sup>a,b,\*</sup>, Zhong Lin Wang<sup>c</sup>

<sup>a</sup>Department of Materials Physics and State Key Laboratory for Advanced Metals and Materials, University of Science and Technology Beijing, Beijing 100083, People's Republic of China

<sup>b</sup>School of Materials Science and Engineering, Georgia Institute of Technology, Atlanta, GA 30332-0245, USA

<sup>c</sup>School of Materials Science and Engineering, Georgia Institute of Technology, 771 Ferst Dr, Atlanta, GA 30332-0245, USA

Received 27 January 2003; accepted 31 March 2003 by D.E. Van Dyck

### Abstract

We have developed a simple solid–vapor approach for controlled growth of the tetraleg ZnO nanostructure at high yield. The length of the tetraleg is 2–3  $\mu\text{m}$  and the edge size of its centering nucleus is 70–200 nm. Our electron microscopy study gives the first direct evidence about the existence of the octahedral multiple twin nucleus, which is confirmed to be responsible for the formation of the tetraleg ZnO nanostructure. The tetraleg ZnO nanostructure is likely to be a candidate as building blocks for constructing photonic crystals.

© 2003 Elsevier Science Ltd. All rights reserved.

PACS: 79.60.Jv; 36.40.–c; 61.46.tw

Keywords: A. Nanostructure; B. Crystal growth

Nanoscale materials exhibit a wide range of electrical and optical properties that depend sensitively on both shape and size, and are of both fundamental and technological interest. One-dimensional (1D) nanostructures, such as nanotubes, nanowires and nanobelts, have attracted extraordinary attention for their potential applications in device and interconnect integration in nanoelectronics and molecular electronics [1–5]. Although different levels of growth controls for nanowires (including positional, orientational, diameter, and density control) have been achieved [6], the shape control of nanostructures is not easily obtained. The synthesis of complex structures of rod-based CdSe nanocrystals e.g. arrow and teardrop, has demonstrated some success in this direction [7–9]. Since the novel properties of nanomaterials depend sensitively on their shape and size, the development of synthetic methods and an understanding of the mechanism by which the shape and size of

nanostructures can be easily controlled is a key issue in nanoscience.

ZnO exhibits a direct bandgap of 3.37 eV at room temperature with a large exciton binding energy of 60 meV. The strong exciton binding energy, which is much larger than that of GaN (25 meV) and the thermal energy at room temperature (26 meV), can ensure an efficient exciton emission at room temperature under low excitation energy [10–11]. As a consequence, ZnO is recognized as a promising photonic material in the blue-UV region. Room temperature UV lasing properties have recently been demonstrated from ZnO epitaxial films, microcrystalline thin films, and nanoclusters [12–15]. The synthesis of 1D single-crystalline ZnO nanostructures has been of growing interest owing to their promising application in nanoscale optoelectronic devices. Single-crystalline ZnO nanowires have been synthesized successfully in several groups [16–20]. Wang et al. reported the synthesis of oxide nanobelts by simply evaporating the commercial metal oxide powders at high temperatures [3,19–20]. The as-synthesized oxide nanobelts are pure, structurally uniform, and single crystalline, and most of them are of free from

\* Corresponding author. Tel.: + 86-10-62332281.

E-mail addresses: [yuezhang@pgschi.ustb.edu.cn](mailto:yuezhang@pgschi.ustb.edu.cn) (Y. Zhang), [daiyingiina@263.net](mailto:daiyingiina@263.net) (Y. Dai).

defects and dislocations. Room temperature UV lasing in ZnO nanowires has been demonstrated very recently [21]. In this paper, we report a simple method for controlled synthesis of a three-dimensional (3D) ZnO nanostructure, called tetraleg ZnO (T-ZnO) nanostructure, by oxidation of Zn powders. The structure of the T-ZnO is fully characterized and a possible growth mechanism is proposed.

The T-ZnO nanostructures were synthesized by thermal evaporation of 99.9% pure zinc powders under controlled conditions without the presence of catalyst. The zinc powders were placed in an alumina crucible that was inserted in a horizontal tube furnace, where the temperature, pressure, and evaporation time were controlled. The temperature of the furnace was ramped to 850–950 °C at a rate of 50–100 °C/min and kept at that temperature for 1–30 min. T-ZnO nanostructures were obtained in the reaction vessel. Structural characterization of the T-ZnO nanostructures were carried out by X-ray diffraction (XRD, D/MAX-RB) with the Cu K $\alpha$  radiation, scanning electron microscopy (SEM, S250-II), transmission electron microscopy (TEM (Hitachi H-800) and High-resolution TEM (HRTEM) (JEM-2010F).

The T-ZnO has a unique structure. Although large size T-ZnO whiskers were reported previously [22–24], the synthesis of nano-size T-ZnO structures in high yield is demonstrated only recently [25]. Fig. 1(a) is a typical SEM images of the T-ZnO nanostructure. The particles are of a tetrahedral shape with four legs. The length of the legs is 2–3  $\mu\text{m}$  and the edge size of the centering nucleus is 70–200 nm. Very little secondary growth components are observed in our synthesis process. Fig. 1(b) is an TEM image of a T-ZnO nanostructure. It is obvious that four legs are extended from the central part. The structure is not single crystalline but composed of several crystalline pieces. A typical XRD pattern of the T-ZnO nanostructures is shown in Fig. 1(c), which proves that the T-ZnO has a wurtzite structure with lattice constants of  $a = 0.324$  nm and  $c = 0.519$  nm. No diffraction peaks from Zn or other impurity phases are found in any of our samples, confirming that the products are pure ZnO.

The detailed structure of individual T-ZnO nanostructure is characterized by TEM. Fig. 2(a) and (b) are bright-field and dark-field images of a T-ZnO nanostructure, respectively. Fig. 2(b) was taken by selecting a diffraction spot coming from the central region of the tetraleg. It is apparent that the center is a distinct grain that is responsible at least in form for the nucleation and growth of the tetraleg structure.

HRTEM observation of the T-ZnO nanostructure is shown in Fig. 3. A low-magnification image given in Fig. 3(a) shows the projected four-fold twin structure at the central region. Fig. 3(b) is a corresponding HRTEM image from the central region. It reveals the structure of the twin boundaries between the element crystals. From the HRTEM image, it can be seen that the interfaces are sharp and show no amorphous layer. These twins are smoothly conjugated fairly coherently at the boundaries with little lattice

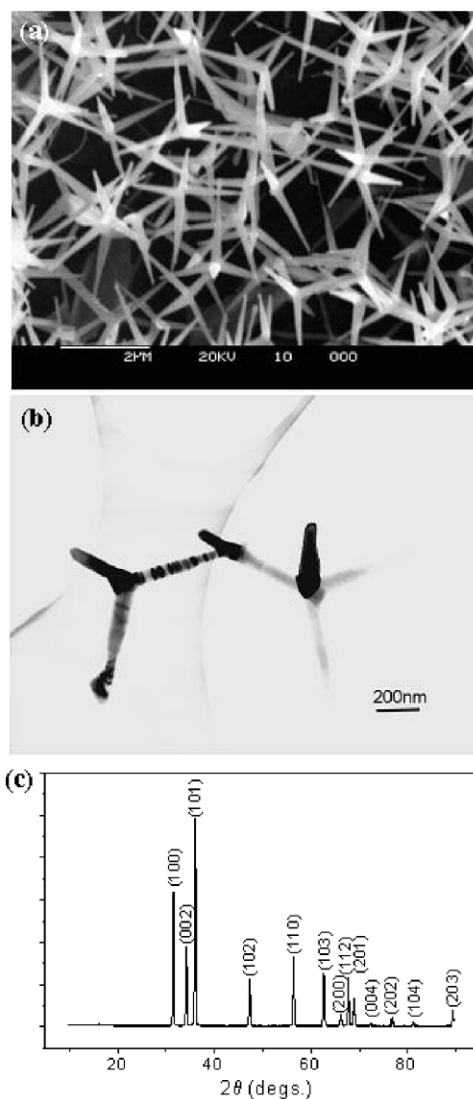


Fig. 1. (a) A typical SEM image showing the general morphology of the tetraleg ZnO nanostructure. (b) An TEM image of the tetraleg structure. (c) XRD pattern from the tetraleg ZnO nanostructure, showing the Wurtzite structure.

distortion. A Fourier transform of Fig. 3(b) is given in Fig. 3(c), based on which the twin planes can be determined to be the  $\{11\bar{2}2\}$  family. The index corresponding the grain at the bottom-left corner of Fig. 3(b) is labeled in Fig. 3(c). The twin plane is indicated by an arrowhead. The incident beam direction is  $[\bar{2}4\bar{2}3]$ , along which the four twin boundaries are imaged edge-on.

The T-ZnO whiskers have stimulated many investigators in the literature to study their structure and growth mechanism. The various models have been proposed for the growth process of the tetrahedral ZnO particles [26–30], but the structure of the T-ZnO whiskers has not been

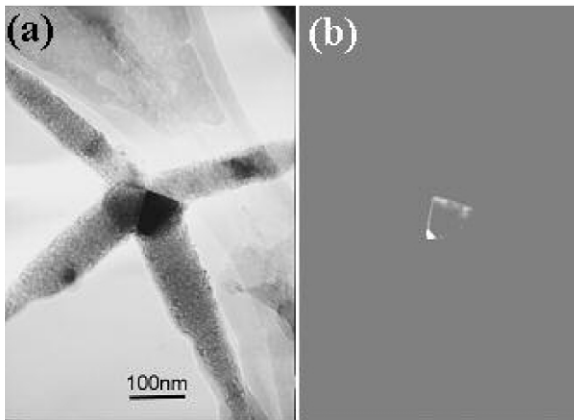


Fig. 2. (a) Bright-field electron micrograph of a tetraleg ZnO nanostructure. (b) A dark-field electron micrograph from the same region, showing a distinct grain at the center, which will be explained by the model presented in Fig. 4(b).

completely determined because the particles investigated by these authors were too large to be identified by TEM. Shioziri suggested that T-ZnO whiskers have the zincblende structure, four wurtzite crystals formed on their (111) faces by introducing stacking faults [26]. Iwanaga proposed the octahedral multiple twin (octa-twin) nucleus models [27]. Nishio proposed a new growth model based on the phase transformation from an octahedral zincblende ZnO crystal to a twinned wurtzite ZnO crystal [28]. Among these models, only the Iwanaga' model (so called octa-twin model) can explain the prototype angle relation. Although his model explained the orientation relationship and the measured angles between the legs matched exactly to that measured from surface morphology, there is no direct evidence in the literature about the existence of the octa-twin nucleus in T-ZnO structure. The nanoscale T-ZnO nanostructures synthesized by us make it possible to directly reveal the structure of the T-ZnO nanostructures by HRTEM for the first time.

The formation of the T-ZnO structure has two stages: nucleation and growth. In our process, nucleation at the initial stage might have a crucial role on the formation of T-ZnO nanostructures. The metallic zinc is in its vapor state at the high temperature (Zn: boiling point of 911 °C). The gaseous zinc diffuse and immediately reoxidize in the environment of oxygen. It is known that the gaseous ZnO only exists as highly activated species with an extremely short lifetime [29]. The oxidation reaction at our processing temperature is as follows:  $2Zn(g) + O_2 = 2ZnO(s)$ . The process of the initial nucleation includes diffusion, collision of atoms and reaction between the vapor molecules (including vapor Zn and  $O_2$ ). When the supersaturation increases to a level at which nuclei formed, the produced ZnO nuclei grow to sizes larger than the critical size. The ZnO nuclei formed in the alumina crucible are homogeneous as carried by the gas phase.

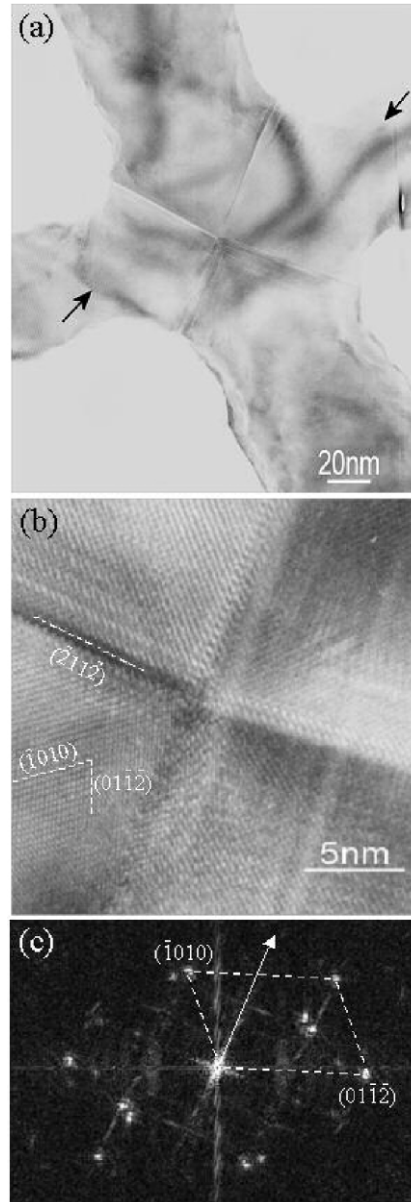


Fig. 3. (a) Low magnification TEM image of a tetraleg ZnO nanostructure. (b) A high-resolution TEM image recorded from the center of the tetraleg structure. (c) A Fourier transform of the image given in (b) and the indexes corresponding to one of the bottom-left grain in (b). The incident beam direction is  $[24\bar{2}3]$ .

According to the octa-twin nucleus model, ZnO nuclei formed in an atmosphere containing oxygen are octa-twins nuclei which consist of eight tetrahedral-shape crystals, each consisting of three  $\{11\bar{2}2\}$  pyramidal facets and one (0001) basal facet (Fig. 4(a)). The eight tetrahedral crystals are connected together by making the pyramidal faces contact one with another to form an octahedron. The surfaces of the octa-twin are all basal planes. An important additional

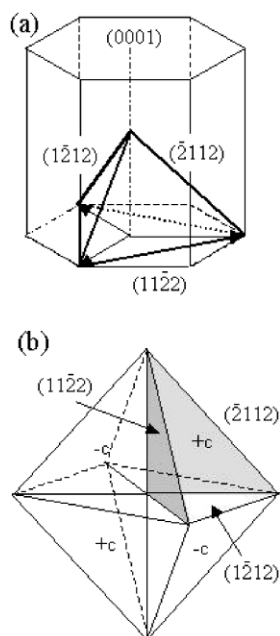


Fig. 4. (a) A pyramid formed by three  $\{11\bar{2}\}$  and one (0001) facets. (b) The octa-twin model composed of eight pyramidal inversion-twin crystals [27].

condition is that every twin is of the inversion type, i.e. the polarities of the twinned crystals are not mirror-symmetric with respect to the contact plane but antisymmetric. Thus the eight basal surfaces of the octa-twin are alternately the plus (0001) surface (+c) and the minus surface (000 $\bar{1}$ ) (-c), as shown in Fig. 4(b). The formation of the tetraleg structure has to do with the following two factors based on the octa-twin nucleus. It is known through the study of ZnO nanowires and nanobelts [3], [0001] is the fastest growth direction in the formation of nanostructure. The octa-twin has four positively charged (0001) surfaces and four negatively charged (000 $\bar{1}$ ) surfaces. The positively charged surfaces are likely to be terminated with Zn, which may be the favorable sites to attracting vapor species, resulting in the growth of whiskers along four [0001] directions that have a geometrical configuration analogous to the diamond bonds in diamond [30]. The growth mechanism is believed to be a solid–vapor process.

Based on the octa-twin model given in Fig. 4(b), the contrast from the ‘extra’ grain shown in the dark-field image in Fig. 2(b) is believed coming from one of the four tetrahedral crystals that is bounded by a negatively charged (000 $\bar{1}$ ) surface, thus, no formation of leg structure.

In summary, we have successfully developed a simple solid–vapor approach to grow the controlled tetraleg ZnO nanostructures. Our experimental observation gives direct evidence about the existence of the octa-twin nucleus, based on which the formation of the T-ZnO nanostructure is

proposed. A high yield production of T-ZnO nanostructures could be important for optoelectronics because they can be used as the fundamental building blocks for constructing photonic crystals.

#### Acknowledgements

The work was supported by the National Natural Science Foundation of China (Grant No. 50172006), the Fund for Returned Overseas Scholar of Ministry of Education of China, the Fund for Cross-Century Talent Projects of Educational Ministry of China, and the Research Fund for the Doctoral Program of Higher Education of China.

#### References

- [1] S. Iijima, *Nature* 354 (1991) 56.
- [2] J. Hu, T.W. Odom, C.M. Lieber, *Acc. Chem. Res.* 32 (1999) 435.
- [3] Z.W. Pan, Z.R. Dai, Z.L. Wang, *Science* 291 (2001) 1947.
- [4] J.R. Heath, P.J. Kuekes, G. Snyder, R.S. Williams, *Science* 280 (1998) 1717.
- [5] D. Snoke, *Science* 273 (1996) 1351.
- [6] P. Yang, H. Yan, S. Mao, R. Russo, J. Johnson, R. Saykally, N. Morris, J. Pham, R. He, H.J. Choi, *Adv. Funct. Mater.* 12 (2002) 323.
- [7] X.G. Peng, L. Manna, W.D. Yang, J. Wickham, E.C. Scher, A. Kadavanich, A.P. Alivisatos, *Nature* 404 (2000) 59.
- [8] L. Manna, E.C. Scher, A.P. Alivisatos, *J. Am. Chem. Soc.* 122 (2000) 12700.
- [9] Y.W. Jun, S.M. Lee, N.J. Kang, J. Cheon, *J. Am. Chem. Soc.* 123 (2001) 5150.
- [10] Y. Chen, D.M. Bagnall, H. Koh, K. Park, K. Hiraga, Z. Zhu, T. Yao, *J. Appl. Phys.* 84 (1998) 3912.
- [11] A. Ohtomo, M. Kawasaki, Y. Sakurai, I. Ohkubo, R. Shiroki, Y. Yoshida, T. Yasuda, Y. Segawa, H. Koinuma, *Mater. Sci. Engng B* 56 (1998) 263.
- [12] D.M. Bagnall, Y.F. Chen, Z. Zhu, T. Yao, S. Koyama, M.Y. Shen, T. Goto, *Appl. Phys. Lett.* 70 (1997) 2230.
- [13] P. Zu, Z.K. Tang, G.K.L. Wong, M. Kawasaki, A. Ohtomo, H. Koinuma, Y. Segawa, *Solid State Commun.* 103 (1997) 459.
- [14] H. Co, J.Y. Xu, E.W. Seelig, R.P.H. Chang, *Appl. Phys. Lett.* 76 (2000) 2997.
- [15] D.Z. Zhang, S.H. Chang, S.T. Ho, E.W. Seelig, X. Liu, R.P.H. Chang, *Phys. Rev. Lett.* 84 (2000) 5584.
- [16] M.H. Huang, Y. Wu, H. Feick, N. Tran, E. Weber, P. Yang, *Adv. Mater.* 13 (2001) 113.
- [17] Y.C. Kong, D.P. Yu, B. Zhang, W. Feng, S.Q. Feng, *Appl. Phys. Lett.* 78 (2001) 407.
- [18] W.I. Park, D.H. Kim, S.W. Jung, G.C. Yi, *Appl. Phys. Lett.* 80 (2002) 4232.
- [19] Z.L. Wang, R.P. Gao, Z.W. Pan, Z.R. Dai, *Adv. Engng Mater.* 3 (2001) 657.
- [20] Z.R. Dai, Z.W. Pan, Z.L. Wang, *Solid State Commun.* 118 (2001) 351.
- [21] M.H. Huang, S. Mao, H. Feick, H. Yan, Y. Wu, H. Kind, E. Weber, R. Russo, P. Yang, *Science* 292 (2001) 1897.

- [22] M.L. Fuller, *J. Appl. Phys.* 15 (1944) 164.
- [23] Y. Suyama, T. Tomokiyo, T. Manabe, E. Tanaka, *J. Am. Ceram. Soc.* 71 (1988) 391.
- [24] H. Iwanaga, M. Fujii, S. Takeuchi, *J. Cryst. Growth* 134 (1993) 275.
- [25] Y. Dai, Y. Zhang, Q.K. Li, C.W. Nan, *Chem. Phys. Lett.* 358 (2002) 83.
- [26] M. Shiojiri, C. Kaito, *J. Cryst. Growth* 52 (1981) 173.
- [27] S. Takeuchi, H. Iwanaga, M. Fujii, *Philos. Mag. A* 69 (1994) 1125.
- [28] K. Nishio, T. Isshiki, *Philos. Mag. A* 76 (1997) 889.
- [29] G.V. Chertihin, L. Andrews, *J. Chem. Phys.* 106 (1997) 3457.
- [30] H. Iwanaga, N. Shibata, O. Nittono, M. Kasuga, *J. Cryst. Growth* 45 (1978) 228.